Two-Band Signal Reconstruction from Periodic Nonuniform Samples

Li Ping Guo[⋆], Chi Wah Kok[†], Hing Cheung So[⋆], Wing Shan Tam[†]
[⋆]*Department of Electronic Engineering*, *City University of Hong Kong*, Kowloon, Hong Kong
[†]*Canaan Semiconductor Limited*, Hong Kong
lpguo2-c@my.cityu.edu.hk, eekok@ieee.org, hcso@ee.cityu.edu.hk, wstam@ieee.org

***Abstract*—The Shannon sampling theorem states the lowest sampling rate for the lowpass bandlimited signals. But for multiband bandlimited signals, it is inefficient to apply the Shannon sampling theorem. This is because the existence of gaps between successive bands makes it possible to realize sampling at a rate, which is lower than the Nyquist rate and lower-bounded by Nyquist-Landau rate. The Nyquist-Landau rate for multiband signals, can be attained via periodic nonuniform sampling. However, it is still very challenging to find the sampling rate for multiband bandlimited signals such that the average sampling rate approaches the Nyquist-Landau rate. In this paper, we aim to find the feasible range of sub-Nyquist sampling rate (such that uniform sampling at this rate causes no aliasing) for two-band signals without aliasing. In this paper, an efficient method to find the constraints on the sampling frequency of two-band signals is devised. The normal placement and inverse placement of the spectrum are considered. Guard bands are considered to increase the robustness of the proposed sampling scheme. Analytical study is provided to obtain the allowable region of sampling frequencies. The derived low sampling rate ensures a relaxed requirement in terms of sampling, processing, and memory.**

***Index Terms*—two-band, reconstruction, periodic nonuniform sampling, sampling frequency range**

I. Introduction

The Shannon sampling theorem addresses reconstructing a lowpass bandlimited signal from its uniform samples. That is, the Nyquist rate, defined to be twice the frequency of the highest frequency component of the continuous-time signal, is the lowest sampling rate that guarantees no spectral aliasing. However, the Nyquist rate of the signal will span into the MHz range if the fundamental frequencies of periodic radio signals are into MHz range [1]. Most analog-to-digital converters (ADCs) either cannot achieve sampling at this high rate or are too expensive [1]. Thus, uniform sampling at the Nyquist rate is not suitable to convert the analog signal to digital domain for further processing. The gaps between consecutive bands make it possible to sample at sub-Nyquist rate which is at least the total bandwidth, namely, the Nyquist-Landau rate [2]. Nevertheless it is difficult to accurately determine the minimum uniform sampling rate of multiband signals with arbitrary band edges [3].

Periodic nonuniform sampling (PNS) is used to obtain a lower average rate [4], [5]. In [6], it has been reported that when sampling the signal using PNS at a rate lower than the Nyquist rate, the original signal can still be exactly recovered. That is, reconstruction can be performed by processing subsamples (obtained nonuniformly) of the original sample sequence at the Nyquist rate [7], [8]. And the average sampling rate can be asymptotically close to the Nyquist-Landau rate when using PNS [6], [9]. The problem of choosing the sampling rate in PNS scheme such that the total rate approaches the Nyquist-Landau rate has not been thoroughly understood however.

Herley and Wong [6] have presented an approach that searches the uniform sampling rate to attain the Nyquist-Landau rate of multiband signals. However, it has many problems in practical implementation such as high computational complexity and possible nonexistence of solution. Our goal in this paper is to design a method to find the range of uniform sampling rate such that no aliasing will be caused at this rate for two-band signals. In so doing, a PNS scheme can be implemented with a sampling scheme that asymptotically achieves the derived sampling rate.

The rest of the paper is organized as follows. PNS is described in Section II. In Section III, we provide an efficient method to find the feasible sampling frequency for normal and inverse spectral placements. A simulation study for a single two-band signal is included in Section IV to verify the effectiveness of our method. Finally, conclusions are drawn in Section V.

II. Periodic nonuniform sampling

PNS is applied to achieve minimal sampling rate that allows the analog signal to be perfectly reconstructed from the corresponding samples. Precisely, several lower-rate discrete signal sequences instead of one high-rate discrete signal sequence are employed in the PNS scheme to realize the reconstruction [10], [11].

Fig. 1 shows the decomposition of one high-rate discrete-time signal into M sampling sequences at rate f_0. The original signal $x(t)$ is first sampled at a rate Mf_0 which is no less than the Nyquist rate. M high-rate sampling sequences are delayed, and then passed through the combination of an M-fold downsampler and an M-fold upsampler. Then, sampling sequences are advanced to be M sampling sequences $x_i[n]$ $(n = 0, \cdots, M-1)$.

A downsampler is an operator that retains only every Mth sample from a sequence, an upsampler inserts $(M-1)$ zero samples between adjacent samples. The effect of the

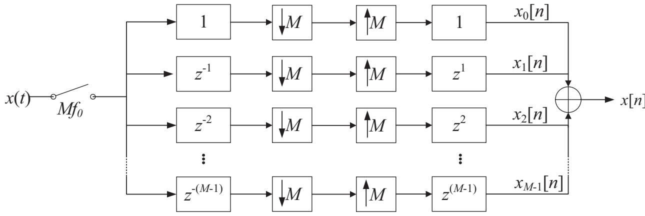

Fig. 1. Sample analog signal $x(t)$ at rate Mf_0 and split it into M signal sequences each with rate f_0.

combination of a downsampler followed by an upsampler is that every Mth sample is retained, while all others are set to zero. Thus the implementation of this sampling strategy is carried by M uniform sequences with sampling rate f_0. Evidently, the average sampling rate is still Mf_0.

The PNS scheme is derived by deleting samples periodically from some uniform sample sequences which means that the samples obtained by PNS are not equally spaced in time. Sampling process is implemented by multiplying the original signal by a periodic uniform impulse sequence with the same sampling period (reciprocal of the sampling rate f_0) [12], which is known as first-order sampling. The spectrum of the sampled sequence consists of replicas of the original signal spectrum shifted by integer times f_0 [13]. More specifically, the spectrum of the sampling signal and the sampling rate are highly correlated. Assume $x(t)$ is a dual-band signal and its Fourier transform $X(f)$ is shown in Fig. 2 (a). Let $X_S(f)$ denote the sampled signal spectrum. When the maximum frequency of the original signal is odd times of $\frac{f_0}{2}$, the sampled signal spectrum looks like Fig. 2 (b). When the maximum frequency of the original signal is even times of $\frac{f_0}{2}$, the sampled signal spectrum looks like Fig. 2 (c).

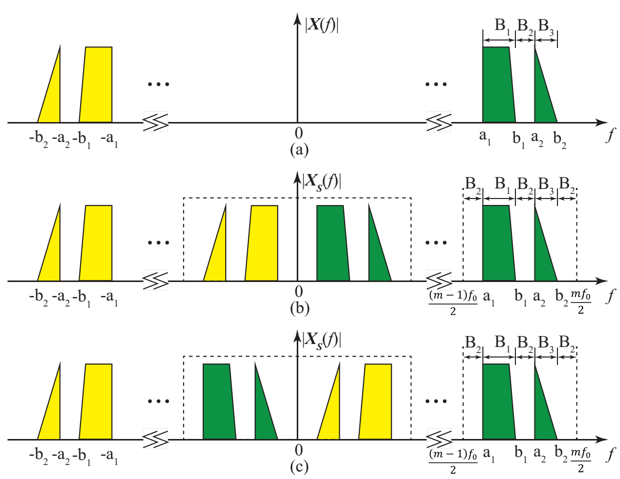

Fig. 2. Signal spectra. (a) Dual-band signal. (b) Sampled signal of normal spectral placement. (c) Sampled signal of inverse spectral placement.

III. Obtaining Valid Sampling Frequency Ranges

The problem that we are considering is to find the constraints on direct sampling frequency of two-band signals, so that no spectral overlapping occurs. To recover correctly the required signal from the discrete signal spectrum, aliasing must be avoided [14]. Due to non-aliasing requirement, many relevant equations for finding the acceptable uniform sampling ranges of a single signal have been suggested [15], [16]. But most results are related to the bandpass case. Although [17] claims to be tackling the multiband case, it only presents a heuristic search technique to find the feasible sampling frequency.

A. Spectral Arrangement after Direct Sampling

For a dual-band signal, there should be 8 possible replica orders when using direct sampling without causing spectral overlapping in the sampled signal spectrum, as discussed in [17]. However, for typical applications, one may find that examining all the possible replica orders eventually ends up with only few valid replica orders, which yield nonempty sampling frequency ranges [17]. In some circumstances, it is not necessary for the sampled signal to possess the same spectral structure as the signal [13]. Thus, we focus on two cases of the arrangement of the shifted replicas of the original spectrum, namely, the normal placement and inverse placement of the spectrum.

B. Sampling Frequencies for Normal and Inverse Placements

Consider the positive spectrum of the multiband signal is placed in the lowest positive part, as shown in the dashed-lined box in Fig. 2 (b). Then the negative spectrum is placed in the lowest negative part. The spectrum in the dashed-lined box possesses the same spectral structure as the original signal spectrum. Then we call this situation the normal spectral placement. Another case is that the positive spectrum of the multiband is placed in the lowest negative part and the negative spectrum is placed in the lowest positive part after sampling, as shown in the dashed-lined box in Fig. 2 (c). The structure in the dashed-lined box is different from the original spectral structure. Then we call this situation the inverse spectral placement. Note that we add guard-bands which equal the intermediate zero bandwidth before and after the spectral bands, in case any engineering imperfection causing sampling frequency change will not generate overlapping aliasing components in practice.

To obtain the conditions for acceptable uniform sampling rates, a complete set of feasible sampling frequencies is derived in the following. To avoid spectrum aliasing of the sampled sequence, the negative and positive parts of the dual-band signal spectrum should be placed alternately. And the supreme number of integer m of the half spectrum, which can be positive and negative spectrum of the dual-band signal in the interval $[0, b_2 + B_2]$, should be limited as

$$m = \left\lfloor \frac{b_2 + B_2}{3B_2 + B_1 + B_3} \right\rfloor = \left\lfloor \frac{b_2 + B_2}{2B_2 + b_2 - a_1} \right\rfloor \qquad (1)$$

Here, we add guard-bands with bandwidth B_2 on the both sides of the positive and negative spectra to increase sampling robustness. Also, to be placed correctly in the normal case, m should be an odd number no less than 1. Similarly, to be placed correctly in the inverse case, m should be even and no less than 2. To avoid aliasing in the case of normal spectral arrangement, the upper limit of the sampling frequency is determined by

$$\frac{(m-1)f_0}{2} \leq a_1 - B_2$$

Thus, we have

$$f_0 \leq \frac{2(a_1 - B_2)}{m-1} \tag{2}$$

and the lower limit of the sampling frequency is determined by

$$\frac{mf_0}{2} \geq b_2 + B_2$$

and we have

$$f_0 \geq \frac{2(b_2 + B_2)}{m} \tag{3}$$

Note that according to the positions of frequency edges, we have $a_1 + B_1 + B_2 + B_3 = b_2$, then the relationship between a_1 and b_2 is obtained as:

$$a_1 \leq b_2 - B_2 \tag{4}$$

Therefore, after combining (2) and (3) the available range of the sampling frequency is

$$\frac{2(b_2 + B_2)}{m} \leq f_0 \leq \frac{2(a_1 - B_2)}{m-1} \tag{5}$$

To show the allowable sampling frequencies with respect to the band positions, we list all the conditions:

$$\begin{cases} \frac{2(b_2+B_2)}{m} \leq f_0 \leq \frac{2(a_1-B_2)}{m-1}, \quad m \in \mathbb{Z}^+ \\ 1 \leq m \leq \left\lfloor \frac{b_2+B_2}{2B_2+b_2-a_1} \right\rfloor \\ a_1 \leq b_2 - B_2 \end{cases} \tag{6}$$

where there are 4 variables for a fixed m. Dividing by B_2 on both sides of the inequality to cut down the variables, we can rewrite (6) to relate the B_2-normalized sampling rate, f_0/B_2, to the B_2-normalized highest frequency component, b_2/B_2 , and so on.

$$\begin{cases} \frac{2}{m} \cdot (\frac{b_2}{B_2}) + \frac{2}{m} \leq \frac{f_0}{B_2} \leq \frac{2}{m-1} \cdot (\frac{a_1}{B_2}) - \frac{2}{m-1}, \quad m \in \mathbb{Z}^+ \\ 1 \leq m \leq \left\lfloor \frac{(\frac{b_2}{B_2})+1}{2+(\frac{b_2}{B_2})-(\frac{a_1}{B_2})} \right\rfloor \\ \frac{a_1}{B_2} \leq \frac{b_2}{B_2} - 1 \end{cases} \tag{7}$$

Then, for a fixed m there are 3 variables, namely, f_0/B_2, b_2/B_2 and a_1/B_2. We draw 3 pictures to illustrate the relationships among them, as shown in Figs. 3 (a), (b) and (c). More clearly, Fig. 3 (a) gives the upper and lower limits of the normalized sampling rate f_0/B_2 with respect to the normalized highest frequency component b_2/B_2 for the values of $m = 1$, 3 and 5. Regions with line pattern represent the acceptable operating points where no aliasing occurs. Similarly, the admissible sampling rates for signal parameter a_1/B_2 are shown in Fig. 3 (b). And the normalized positions of a_1 and b_2 need to satisfy the constraint are shown in Fig. 3 (c).

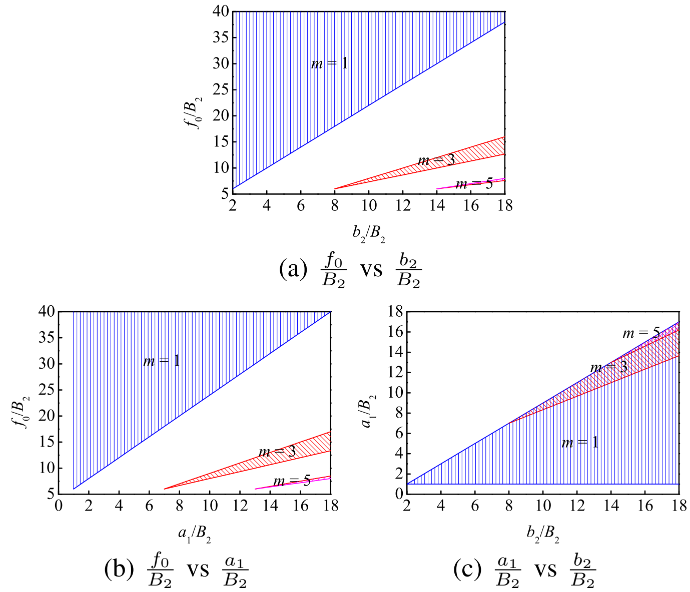

(a) $\frac{f_0}{B_2}$ vs $\frac{b_2}{B_2}$

(b) $\frac{f_0}{B_2}$ vs $\frac{a_1}{B_2}$

(c) $\frac{a_1}{B_2}$ vs $\frac{b_2}{B_2}$

Fig. 3. Allowable regions (shaded regions) of normal spectral placement.

With the same way, we depict allowable region of sampling frequencies for values of $m = 2$, 4 and 6 in Figs. 4 (a), (b) and (c), in which the sampling frequencies and positions of the signal are normalised by B_2. Aliasing can be avoided as long as the sampling rate lies within the acceptable ranges of Figs. 4 (a) and (b).

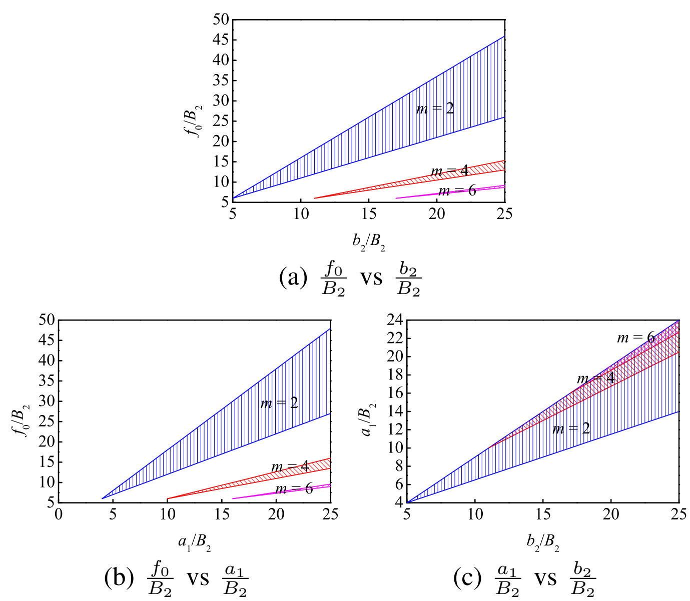

(a) $\frac{f_0}{B_2}$ vs $\frac{b_2}{B_2}$

(b) $\frac{f_0}{B_2}$ vs $\frac{a_1}{B_2}$

(c) $\frac{a_1}{B_2}$ vs $\frac{b_2}{B_2}$

Fig. 4. Allowable regions (shaded regions) of inverse spectral placement.

In principle, we can sample the signal as low as the theoretical minimum (the tip of one of shaded regions in Figs.

3 (a) and (b). But in practice, real-world devices have sampling frequency fluctuations, such as lasers and ADCs [18]. The frequency fluctuation can lead to a new operating point, which is slightly different from the initially selected one. For example, the ADC clock jitter would cause vertical movement of the operating point. The change may cause aliasing when the operating point is not in the non-aliasing regions, where the aliasing regions are in between. In the case of big supreme number, where the non-aliasing region is very narrow, the problem becomes even worse. To avoid this problem, we need to use devices with high stability. Thus the implementation of choosing the operating point must depend on the device specifications. That is why we need to choose different values of m to calculate the range of f_0.

IV. Simulation results

A mathematical expression for our studied two-band signal is given by

$$x(t) = x_1(t) + x_2(t) = \sum_{i=1}^{2} B_i \mathrm{sinc}(B_i t) \cdot 2\cos(2\pi f_i t) \quad (8)$$

where B_i is the right-side bandwidth of real-valued signal $x_i(t) = B_i \mathrm{sinc}(B_i t) \cdot 2\cos(2\pi f_i t)$ and we set $B_1 = 20$MHz, $B_2 = 40$MHz, $f_1 = 200$MHz, $f_2 = 240$MHz. The signal and its frequency spectrum are shown in Fig. 5.

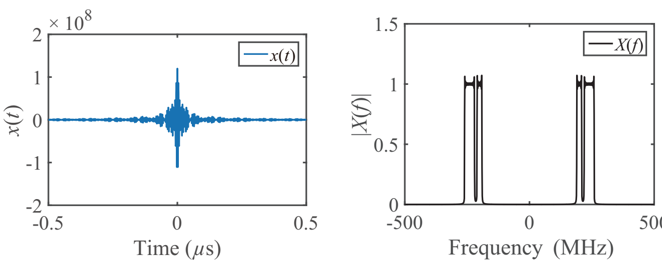

(a) Original signal (b) Frequency spectrum

Fig. 5. A two-band signal in time domain (a) and frequency domain (b).

When using the method in Section III, the minimum value of sampling frequency f_0 is 180MHz. After sampling the signal at rate $f_0 = 180$ MHz, we get a discrete-time signal as shown in Fig. 6 (a). And the frequency spectrum with the normalized magnitude at the interval $[-f_0/2, f_0/2]$ is shown in Fig. 6 (b). It is seen that there are no overlaps in the frequency spectrum after sampling with the specific sampling frequency and the sampling frequency is far less than the Nyquist rate 520MHz. Hence PNS can be implemented with this sampling rate.

The actual signal generated by white Gaussian noise with a pulse shape filtering is used to verify the proposed method. The ideal filter is the same as Fig. 5 (b). The Parks-McClellan algorithm is used to design a linear phase and casual finite impulse response digital filter to approximate the ideal filter. We specify the two passbands to extend from 193 to 207, and 224 to 260 MHz, respectively. The two stopbands extend from 0 to 187 and 213 to 216 MHz. A maximum stopband

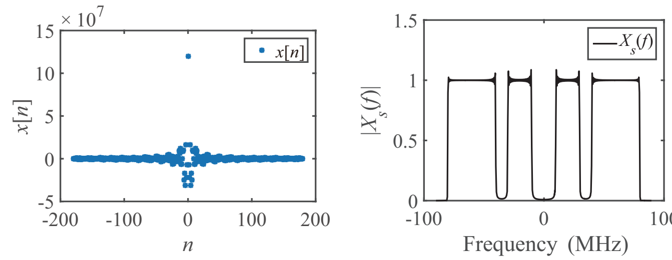

(a) Sampled signal (b) Frequency spectrum

Fig. 6. Sampled signal with sampling rate $f_0 = 180$MHz.

amplitude of 0.001 and a maximum passband error (ripple) of 0.0012 are specified. 1000 real-valued white Gaussian noise samples with power 0 dBW are generated. According to our method, the sampling rate should be 180 MHz. After sampling, the estimated power spectral density (PSD) with respect to the frequency is shown in Fig. 7.

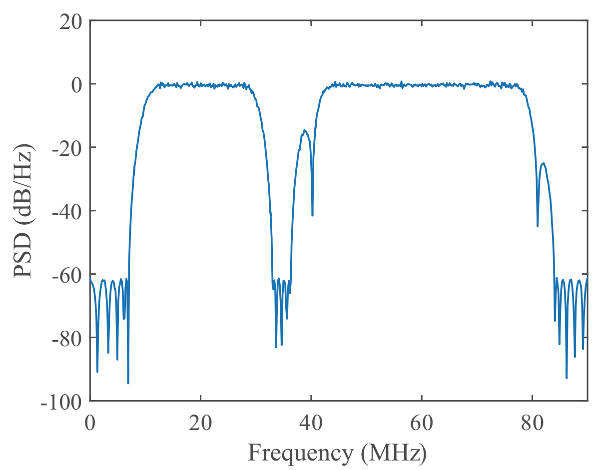

Fig. 7. Estimated power spectral density.

V. Conclusion

In this paper, the problem of finding the complete set of feasible sampling rate of two-band signals when using the PNS scheme has been solved. The sampling rate is far less than the Nyquist rate and guarantees no spectral aliasing. And the allowable regions of sampling rate with respect to different band edges have been obtained. Also, guard-bands are added before and after the spectral bands which increase the robustness of the sampling scheme. Then different sampling frequency can be chosen depending on individual application requirements. Moreover, we take an example for a two-band signal to verify the effectiveness of the proposed approach.

REFERENCES

[1] F. Papenfuss and D. Timmermann, "Alias-free periodic signal analysis using efficient rate nonuniform sampling sets," in *Proceedings of IEEE International Conference on Acoustics, Speech and Signal Processing*, Honolulu, HI, USA, Apr. 2007, vol. 3, pp. 1497–1500.

[2] M. Rashidi and S. Mansouri, "Parameter selection in periodic nonuniform sampling of multiband signals," in *Proceedings of International Symposium on Electrical and Electronics Engineering*, Galati, Romania, Sep. 2010, pp. 79–83.

[3] B. Foster and C. Herley, "Exact reconstruction from periodic nonuniform samples," in *Proceedings of IEEE International Conference on Acoustics, Speech, and Signal Processing*, Detroit, MI, USA, May 1995, vol. 2, pp. 1452–1455.

[4] S.C. Scoular and W.J. Fitzgerald, "Periodic nonuniform sampling of multiband signals," *Signal Processing*, vol. 28, no. 2, pp. 195–200, 1992.

[5] B. Foster and C. Herley, "Exact reconstruction from periodic nonuniform sampling of signals with arbitrary frequency support," in *Proceedings of IEEE International Conference on Acoustics, Speech and Signal Processing*, Seattle, WA, USA, May 1998.

[6] C. Herley and P.W. Wong, "Minimum rate sampling and reconstruction of signals with arbitrary frequency support," *IEEE Transactions on Information Theory*, vol. 45, no. 5, pp. 1555–1564, Jul. 1999.

[7] R. Venkataramani and Y. Bresler, "Perfect reconstruction formulas and bounds on aliasing error in sub-nyquist nonuniform sampling of multiband signals," *IEEE Transactions on Information Theory*, vol. 46, no. 6, pp. 2173–2183, Sep. 2000.

[8] E. Mohammadi and F. Marvasti, "Sampling and distortion tradeoffs for bandlimited periodic signals," *IEEE Transactions on Information Theory*, vol. 64, no. 3, pp. 1706–1724, Mar. 2018.

[9] H.J. Landau, "Necessary density conditions for sampling and interpolation of certain entire functions," *Acta Mathematica*, vol. 117, no. 1, pp. 37–52, Feb. 1967.

[10] T. Moon, H.W. Choi, N. Tzou, and A. Chatterjee, "Wideband sparse signal acquisition with dual-rate time-interleaved undersampling hardware and multicoset signal reconstruction algorithms," *IEEE Transactions on Signal Processing*, vol. 63, no. 24, pp. 6486–6497, Dec. 2015.

[11] J. Janczak and E. Pawluszewicz, "Exponential stability of systems under periodic sampling of the second order," in *Proceedings of International Conference on Methods and Models in Automation and Robotics*, Miedzyzdroje, Poland, Aug. 2017, pp. 514–518.

[12] J.H. Liu and X.Y. Zhou, "Spectrum arrangement and the generalized bandpass signal direct sampling theorem," in *Proceedings of Third International Conference on Signal Processing*, Beijing, China, Oct. 1996, vol. 1, pp. 28–31.

[13] J.H. Liu, X.Y. Zhou, and Y.N. Peng, "Spectral arrangement and other topics in first-order bandpass sampling theory," *IEEE Transactions on Signal Processing*, vol. 49, no. 6, pp. 1260–1263, Jun. 2001.

[14] J. Bae and J. Park, "A searching algorithm for minimum bandpass sampling frequency in simultaneous down-conversion of multiple RF signals," *Journal of Communications and Networks*, vol. 10, no. 1, pp. 55–62, Mar. 2008.

[15] J.-C. Liu, "Bandpass sampling of multiple single sideband RF signals," in *Proceedings of International Symposium on Communications, Control and Signal Processing*, St Julians, Malta, Mar. 2008, pp. 863–866.

[16] M. Mishali and Y.C. Eldar, "Sub-Nyquist sampling," *IEEE Signal Processing Magazine*, vol. 28, no. 6, pp. 98–124, Nov. 2011.

[17] C.-H. Tseng and S.-C. Chou, "Direct downconversion of multiband RF signals using bandpass sampling," *IEEE Transactions on Wireless Communications*, vol. 5, no. 1, pp. 72–76, Jan. 2006.

[18] P. Bakopoulos, S. Dris, B. Schrenk, I. Lazarou, and H. Avramopoulos, "Bandpass sampling in heterodyne receivers for coherent optical access networks," *Optics Express*, vol. 20, no. 28, pp. 29404–29412, Dec. 2012.